SUPPLEMENTAL MATERIAL

1. Materials and methods

Materials

AM251, AM630, anandamide (AEA), and (-)-cannabidiol (CBD) were purchased from Cayman Chemical Company; AMG 9810, γ-irradiated lipopolysaccharides from *Escherichia coli* 026:B6 (LPS), lipoteichoic acid from *Staphylococcus aureus* (LTA), arachidonic acid (AA), capsazepine (CPZ), cyclosporine A (CSA), GF109203X (GF), GSK1016790A (GSK), H89, linoleic acid (LA), ruthenium red (RR) and testosterone (T) were obtained from Sigma-Aldrich. HC067047 (HC) was purchased from Maybridge Ltd., ZM241385 (ZM) from Tocris Bioscience, and Gö6976 (Gö) and wortmannin (WM) from Calbiochem. AA, AEA, AM251, CBD and LA were dissolved in absolute ethanol (Sigma-Aldrich), while the solvent for AM630, AMG 9810, CBD (only in hSOC experiments), CPZ, CSA, GF, Gö, GSK, HC, RR, T, WM and ZM was DMSO (Sigma-Aldrich). LPS, LTA and H89 were dissolved in filtered distilled water.

Cell culturing

Human immortalized SZ95 sebocytes, originated from human facial sebaceous glands (19), were cultured in Sebomed® Basal Medium (Biochrom) supplemented with 10% fetal bovine serum (LifeTechnologies), 1 mM $CaCl_2$, 5 ng/ml human epidermal growth factor (Sigma-Aldrich), 50 IU/ml penicillin and 50 µg/ml streptomycin (both from Teva). The final calcium concentration of the medium was approximately 1.25 mM ("high-Ca^{2+} medium"). The "low-Ca^{2+} Sebomed medium" was prepared to set the Ca^{2+} concentration to 0.25 mM. The medium was changed every other day, and cells were sub-cultured at 60-70% confluence.

Determination of intracellular lipids

For semi-quantitative detection of sebaceous lipids, cells were cultured on glass coverslips, and treated with various compounds for 24 hrs. Cells were then washed in phosphate-buffered saline (PBS; 115 mM NaCl, 20 mM Na_2HPO_4, pH 7.4; all from Sigma-Aldrich), fixed in 4% paraformaldehyde/PBS (Sigma-Aldrich), washed again twice in PBS and once in 60% isopropanol, and stained in freshly prepared Oil Red O solution (in 60% isopropanol) (Sigma-Aldrich) for 20 minutes at 37°C. Nuclei were counterstained with Mayer's hematoxylin (Sigma-Aldrich) for 20 s and coverslips were finally mounted in mounting medium (DAKO).

For quantitative measurement of lipid content, cells (densities: 2,000 cells/well [6-day treatments] or 20,000 cells/well [24-48-hr treatments]) were cultured in 96-well black-

well/clear-bottom plates (Greiner Bio-One) in quadruplicates, and were treated with compounds as indicated. Subsequently, supernatants were discarded, cells were washed twice with PBS, and 100 µl of a 1 µg/ml Nile Red (Sigma-Aldrich) solution in PBS was added to each well. The plates were then incubated at 37°C for 20 min, and fluorescence was measured on a Molecular Devices FlexStation^{384} II or FlexStation 3 **FL**uorescence **I**mage Micro**P**late **R**eader (**FLIPR**; Molecular Devices). Results are expressed as percentages of the relative fluorescence units (RF) in comparison with the controls using 485 nm excitation and 565 nm emission wavelengths for neutral lipids, and 540 nm excitation and 620 nm emission wavelengths for polar lipids.

Investigation of the lipidome

Chemicals

Eluents and extraction solvents were of HPLC/MS grade and were purchased from Merck. Ammonium formate (HCOONH4) was of HPLC/MS grade and was purchased in granular form from Fluka. The authentic triglycerides (TG) 1-palmitoyl-2-oleoyl-3-lineoleoyl-rac-glycerol and 1,3-dipalmitoyl-2-oleoylglycerol were purchased from Cayman Chemical Company and Sigma-Aldrich, respectively. The authentic diacylglyceride (DG) 1,2-dioleoyl-sn-glycerol was purchased from Cayman. The authentic free fatty acids (FFA) linoleic, palmitoleic, palmitic, stearic, oleic, linolenic, and arachidonic acids, as well as the standard wax ester (WE) lauryl palmitoleate, and the standard squalene (SQ), free cholesterol (CH) and cholesteryl esters (CE) oleate, linoleate, and arachidonate were purchased from Sigma-Aldrich. Dodecanoyl sphingomyelin (12:0 SM) was purchased from Avanti Polar Lipids, and used as the internal standard.

Sample extraction

SZ95 sebocytes were harvested by trypsinization and counted. Before extraction, cell pellets were suspended in 500 µl of 5 mM ammonium formate. Extraction of neutral lipids was performed as previously described with slight modifications (78). 500 µl of abs. EtOH and 500 pM of the internal standard 12:0 SM were added to the cell suspension and mixed thoroughly. Liquid-liquid extraction was performed twice with 3 ml EtOAc. The unified layers of EtOAc were evaporated under a gentle stream of nitrogen. The total lipid extract was dissolved in Ac_2O/MeOH/iPrOH 40/40/20 before injection.

LC-MS analysis of lipid extracts

The lipid extracts were analyzed as previously reported (78). Shortly, the rapid resolution reversed phase HPLC (RR-RP-HPLC) separation was performed with Zorbax SB-C8 stationary phase. Lipids were eluted with a binary gradient of (A) 5 mM ammonium formate in MilliQ water (18.2 Ω) and (B) MeOH/iPrOH 95/5. The eluent outlet was connected to a G6220A series time of flight mass spectrometer (ToF-MS, Agilent Technologies) by means of electrospray ionization (ESI) interface

operating in the positive and negative ion modes. Neutral lipids and free fatty acids were detected in the positive and the negative ion mode, respectively. Scan mode ToF mass spectra were acquired in the positive and negative ion mode by using the ToF at 10,000 mass resolving power for scans over the range from m/z 100 to m/z 1000. MS scans were processed using the Mass Hunter software (B.01.03 version). The resulting data were converted to mass centroid from which the accurate m/z value was measured. Accurate mass measurements and isotopic patterns were the basis to retrieve the elemental composition and unsaturation degree of detected compounds. Identity of lipid species was established with the previously reported methodology (78).

Data extraction and statistical analysis

Following the RR-RP-HPLC separation, retention times of neutral and acidic lipids that were expected to be present in the SZ95 sebocyte lipid extracts were consistent with those of authentic standards and with our previous findings. Peak areas of the individual lipids detected in the positive and negative ion modes were obtained from extracted ion chromatograms (EIC) derived by extraction of the m/z values of their pseudomolecular ion (78). To determine the relative abundance of neutral lipids the peak area of individual lipid species detected in the positive ion mode was normalized by the cell number and the peak area of the internal standard 12:0 SM in the EIC obtained by extraction of the m/z 647.5128 corresponding to the [M+H]+ ion C35H72N2O6P. To determine the relative abundance of FFA, which were detected in the negative ion mode, their peak area was normalized by the cell number and the peak area of the internal standard 12:0 SM in the EIC obtained by extraction of the m/z 691.5032 corresponding to the [M+HCOO]- ion C36H72N2O8P of the internal standard. Total relative abundance of lipid groups, i.e. TG, DG, WE, CE, and FFA was obtained by summing the relative abundance of individual lipids belonging to the same lipid class.

Determination of cellular viability

The viability of the cells was determined by measuring the conversion of the tetrazolium salt MTT (Sigma-Aldrich) to formazan by mitochondrial dehydrogenases. Cells were plated in 96-well plates (densities: 2,000 cells/well [6-day treatments] or 20,000 cells/well [2-day treatments]) in quadruplicates, and were cultured for 2 or 6 days. Cells were then incubated with 0.5 mg/ml MTT for 2 hrs, and concentration of formazan crystals (as an indicator of number of viable cells) was determined colorimetrically as described previously (10, 12). Results were expressed as percentage of vehicle controls regarded as 100%.

Determination of apoptosis

A decrease in the mitochondrial membrane potential is one of the earliest markers of apoptosis. Therefore, to assess the process, mitochondrial membrane potential of SZ95 sebocytes was determined using a MitoProbe™ $DiIC_1(5)$ Assay Kit (Life Technologies). Cells (20,000 cells/well) were cultured in 96-well black-well/clear-bottom plates (Greiner Bio One) in quadruplicates and were treated with various compounds for 24 hrs. After removal of supernatants, cells were incubated for 30 minutes with $DiIC_1(5)$ working solution (50 µl/well), then washed with PBS, and the fluorescence of $DiIC_1(5)$ was measured at 630 nm excitation and 670 nm emission wavelengths using the above FLIPRs (Molecular Devices). RF values were expressed as percentage of vehicle controls regarded as 100%.

Determination of necrosis

Necrotic processes were determined by SYTOX Green staining (Life Technologies). The dye is able to penetrate (and then bind to the nucleic acids) only to necrotic cells with ruptured plasma membranes, whereas healthy cells with intact surface membranes show negligible SYTOX Green staining. Cells were cultured in 96-well black-well/clear-bottom plates (Greiner Bio One), and treated with CBD for up to 24 hrs. Supernatants were then discarded, and the cells were incubated for 30 minutes with 1 µM SYTOX Green dye. Following incubation, cells were washed with PBS, the culture medium was replaced, and fluorescence of SYTOX Green was measured at 490 nm excitation and 520 nm emission wavelengths using FLIPR (Molecular Devices).

Determination of cellular proliferation

The degree of cellular growth (reflecting proliferation) was determined by measuring the DNA content of cells using CyQUANT Cell Proliferation Assay Kit (Life Technologies). SZ95 sebocytes (5,000 cells per well) were cultured in 96-well black-well/clear-bottom plates (Greiner Bio-One) and were treated as indicated for 24, 48 and 72 hrs. Supernatants were then removed by blotting on paper towels, and the plates were subsequently frozen at -80°C. The plates were then thawed at room temperature, and 200 µl of CyQUANT dye/cell lysis buffer mixture was added to each well. After 5 minutes of incubation, fluorescence was measured at 490 nm excitation and 520 nm emission wavelengths using FLIPR (Molecular Devices).

RNA isolation, reverse transcription, quantitative "real-time" PCR (Q-PCR)

Q-PCR was performed on an ABI Prism 7000 sequence detection system (Applied Biosystems) or Stratagene Mx3005P QPCR System (Agilent Technologies) using the 5' nuclease assay. Total RNA was isolated using TRIzol (LifeTechnologies), DNase

treatment was performed according to the manufacturer's protocol, and then 1 µg of total RNA were reverse-transcribed into cDNA by using 15 IU of AMV reverse transcriptase (Promega) and 0.025 µg/µl random primers (Promega). PCR amplification was performed by using the TaqMan primers and probes (assay ID-s: Hs00189038_m1 for cathelicidin, Hs00174097_m1 for *IL1B*, Hs00985639_m1 for *IL6*, Hs01032443_m1 for Ki67 (*MKI67*), Hs00942766_s1 for *NRIP1*, Hs01082394_m1 for *TRIB3*, Hs00261256_m1 for *ARHGAP9*, Hs00169123_m1 for A2a receptor (*ADORA2A*), Hs00174128_m1 for *TNFA*, Hs00218912_m1 for *TRPV1*, Hs00275032_m1 for *TRPV2*, Hs00222101_m1 for *TRPV4*, Hs00175798_m1 for *TRPA1* and Hs00375481_m1 for *TRPM8*) and the TaqMan universal PCR master mix protocol (Applied Biosystems). As internal controls, transcripts of glyceraldehyde 3-phosphate dehydrogenase (*GAPDH*), peptidyl-prolyl isomerase A (cyclophilin A; *PPIA*), and 18S ribosomal RNA (*18S*) were determined (assay ID-s: Hs99999905_m1, Hs 99999904_m1, and Hs99999901_s1, respectively). The amount of the transcripts was normalized to those of the relevant housekeeping gene using the ΔCT method. When indicated, the results were then normalized to the expression of the vehicle control (ΔΔCT method).

Immunocytochemistry

SZ95 sebocytes, seeded and cultured on sterile coverslips in 24-well plates, were fixed in ice-cold acetone for 5 min and then permeabilized by 0.1% Triton-X-100 (Sigma-Aldrich) in PBS for 10 min. After washing in PBS and blocking in 1% BSA (Sigma-Aldrich) in PBS for 30 min, cells were incubated with the TRPV1 (Sigma-Aldrich), TRPV2, TRPA1, TRPM8, A2a (AbCam) and TRPV4 (Alomone Labs) specific primary antibodies (all produced in rabbit; dilution 1:500 in blocking solution; overnight incubation at 4°C). For fluorescence staining, slides were then incubated with Alexa-Fluor®-488-conjugated rabbit IgG Fc segment-specific secondary antibodies (developed in goat; Life Technologies) for 60 min (dilution 1:200), and the nuclei of cells were visualized using DAPI (Vector Laboratories). Cells were examined on a Nikon Eclipse E600 fluorescent microscope (Nikon). As negative controls, the appropriate primary antibodies were omitted from the procedure.

Western blotting

Cells were harvested in lysis buffer (20 mM Tris-HCl, pH 7.4, 5 mM EGTA, 1 mM 4-(2-aminoethyl)benzensulfonyl fluoride, protease inhibitor cocktail diluted 1:100, all from Sigma-Aldrich) and the protein content was measured by a modified BCA protein assay (Pierce). The samples were then subjected to sodium dodecyl sulfate-polyacrylamide gel electrophoresis (7.5% gels were loaded with equal [20-60 µg] amount of protein per lane), transferred to BioBond nitrocellulose membranes (Whatman), and then probed with rabbit-anti-human NRIP1 and TRIB3 (both from

Novus Biologicals; 1:200 dilution in 5% milk containing PBS), rabbit-anti-human MAPK ERK1/2, mouse-anti-human P-ERK1/2 (both from Santa Cruz; 1:1500 dilution in both cases in 5% milk containing PBS), mouse-anti-human P-IκBα (Cell Signaling; 1:1000 dilution in 5% milk containing PBS), rabbit-anti-P-P65 (Novus Biologicals; 1:1000 dilution in 5% milk containing PBS) or the above primary anti-TRP channel and anti-A2a receptor specific antibodies (all of them were applied in 1:200 in 5% milk containing PBS). As secondary antibodies, horseradish peroxidase-conjugated rabbit or mouse IgG Fc segment-specific antibodies (developed in goat and sheep, respectively, 1:1000, Bio-Rad) were used, and the immunoreactive bands were visualized by a SuperSignal® West Pico Chemiluminescent Substrate enhanced chemiluminescence kit (Pierce) using a KODAK Gel Logic 1500 Imaging System (Eastman Kodak Company). To assess equal loading, when indicated, membranes were re-probed with anti-β-actin antibodies and visualized as described above.

Semiquantitative densitometric analysis of the signals was performed by using Image J software (NIH).

Full-thickness human skin organ culture and sample preparations

Sample preparation and organ culture

4 mm biopsies of intact human scalp and arm skin samples obtained from 4 female individuals (average age: 56 years old) were punched out using a biopsy punch (pfm medical). These biopsies were maintained in serum-free William's E medium (Biochrom) supplemented with 2 mM L-glutamine (Life Technologies), 10 ng/ml hydrocortisone (Sigma-Aldrich), 10 µg/ml insulin (Sigma-Aldrich), and 1% antibiotic/antimycotic mixture (PAA Laboratories GmbH). The control group received vehicle alone. The skin biopsies were left to float in the medium, with the epidermis up at the air/liquid interface and the dermis/subcutis down (20). The cultures were incubated at 37°C in a gassed incubator with 95% air and 5% CO_2 at 37°C.

Oil Red O staining

After the organ culture, skin samples were embedded in Cryomatrix (Thermo Shandon Limited) and frozen in liquid nitrogen. Cryo-sections of 6 µm thickness were processed for Oil red O histochemistry. After washing in distilled water, cryo-sections were incubated in 60% isopropanol (Sigma-Aldrich), and stained in freshly prepared Oil Red O solution (0.3% in isopropanol; Sigma-Aldrich). Nuclei were counterstained with hematoxylin (Carl Roth GmbH) and the sections were mounted in aqueous mounting medium (DAKO). Images were analyzed by Image J image analysis software (NIH).

MKI67 staining

To assess proliferation in human skin organ cultures, a MKI67 staining method was employed. Briefly, after CBD treatment, cryostat sections were labeled with a mouse anti-MKI67 antiserum (1:20, DAKO). MKI67-positive cells were visualized by using a rhodamine-conjugated goat anti-mouse secondary antibody (1:200, Jackson ImmunoResearch). Sections were then counterstained with DAPI (4',6-diamidino-2-phenylindole; Vector Laboratories). The analysis for cell counting on 2 sections per group was performed using a fluorescence microscope BZ-8100 (Biozero, Keyence). The distance between two analyzed sections was more than 50 µm.

RNA interference (RNA_i)

RNAi was performed according to our optimized protocols (10, 38). In brief, SZ95 sebocytes at 50-70% confluence were transfected with specific Stealth RNAi oligonucleotides (40 nM) against NRIP1 (ID-s: HSS112045 ("siNRIP1a") and HSS112046 ("siNRIP1b")), TRIB3 (ID-s: HSS184051 ("siTRIB3a") and HSS184052 ("siTRIB3b"), TRPV1 (ID-s: HSS111304 ("sV1a") and HSS111306 ("siV1b")), TRPV2 (ID-s: HSS122144 ("siV2a") and HSS122145 ("siV2b")) and TRPV4 (ID-s: HSS126973 ("siV4a") and HSS126974 ("siV4b")) using Lipofectamine 2000 (all from Life Technologies). For controls, RNAi Negative Control Duplexes (Scrambled RNAi "medium") were applied. The efficacy of RNAi-driven "knock-down" was evaluated daily by Western blotting and by Q-PCR.

Microarray analysis

Gene expression analysis of three independent sets of control and CBD-treated SZ95 sebocytes (10 µM CBD for 24 hrs) was performed by using Human Whole Genome Oligo Microarray® (44K) (Agilent Technologies). Total RNA was isolated using TRIzol (LifeTechnologies) according to the manufacturer's protocol, and the isolated RNA was quality-checked by Agilent 2100 Bioanalyzer platform (Agilent Technologies) and Nanodrop-1000 Spectrophotometer (NanoDrop/Thermo Scientific). Alterations in the gene expression were regarded as significant if (i) there were at least two-fold changes in the corresponding levels; (ii) the changes were equi-directional in all cases; and (iii) global, corrected *P* value was less than 0.05. Evaluation, Gene Set Enrichment Analysis (GSEA) and Biological Networks Gene Ontology analysis (BiNGO) of the results was performed by Abiomics Ltd (http://www.abiomics.eu).

Data have been deposited in NCBI's Gene Expression Omnibus (79) and are accessible through GEO Series accession number GSE57571 (http://www.ncbi.nlm.nih.gov/geo/query/acc.cgi?acc=GSE57571).

Determination of the intracellular 3'-5'-cyclic adenosine monophosphate concentration (cAMP ELISA)

SZ95 sebocytes were treated for 1 hour with vehicle or CBD (10 µM). Cells were then lysed (cell density: 10^7 cells/ml), and cell lysates were assayed immediately according to the manufacturer's protocol, using Parameter Cyclic AMP Assay (R&D Systems). Evaluation of the data was performed by using "Four Parameter Logistic Curve" online data analysis tool of MyAssays Ltd. (http://www.myassays.com/four-parameter-logistic-curve.assay).

Patch-clamp recording

Whole cell patch clamp measurements were made by using an Axopatch 200A amplifier and Clampex 10.0 software (Molecular Devices) or an EPC-10 amplifier and Patchmaster software (HEKA Elektronik). To record CBD evoked transmembrane currents, experiments were performed in normal Ringer solution (in mM: NaCl, 140; KCl, 5; glucose, 10; HEPES, 10; $CaCl_2$, 2; $MgCl_2$, 1; and sodium-pyruvate, 1; pH 7.2) and patch pipettes were filled with a solution containing (in mM): K-gluconate, 120; NaCl, 5; 4-(2-hydroxyethyl)-1- piperazineethanesulfonic acid (HEPES), 10; EGTA, 2; $CaCl_2$, 0.1; Mg-ATP, 5; Na_3-GTP, 0.3; Na_2-phosphocreatinine, 10; pH 7.3. To record TRPV4 current, the bath solution consisted of 150 mM NaCl, 6 mM CsCl, 5 mM $CaCl_2$, 1 mM $MgCl_2$, 10 mM HEPES and 10 mM glucose buffered to pH 7.4 (NaOH), whereas the pipette solution consisted of 100 mM aspartic acid, 20 mM CsCl, 1 mM $MgCl_2$, 0.08 mM $CaCl_2$, 4 mM Na_2ATP, 10 mM BAPTA, 10 mM HEPES and pH was set to 7.2 using CsOH resulted in ca. 100 mM CsAsp in the final pipette solution. The holding potential was 0 mV and cells were ramped every 2 s from −120 to +100 mV over the course of 400 ms.

Fluorescent Ca^{2+}-imaging

Fluorescent Ca^{2+}-imaging was performed according to our previously optimized protocol (80). In brief, SZ95 sebocytes were seeded in 96-well black-well/clear-bottom plates (Greiner Bio-One) at a density of 20,000 cells per well. Cells were washed two times with 1% bovine serum albumin (Sigma-Aldrich) and 2.5 mM Probenecid (Sigma-Aldrich) containing Hank's solution (136.8 mM NaCl, 5.4 mM KCl, 0.34 mM Na_2HPO_4, 0.44 mM KH_2PO_4, 0.81 mM $MgSO_4$, 1.26 mM $CaCl_2$, 5.56 mM glucose, 4.17 mM $NaHCO_3$, pH 7.2, all from Sigma-Aldrich). The cells were then incubated with 1 µM Fluo-4 AM (Life Technologies) containing Hank's solution (100 µl/well) at 37°C for 30 min, and were then washed three times with Hank's solution (100 µl/well; in the case of the "low Ca^{2+} Hank" the $CaCl_2$ content was supplemented by equimolar glucose). The plates were then placed in a FLIPR (Molecular Devices), and changes in $[Ca^{2+}]_{IC}$ (reflected by changes fluorescence; excitation: 490 nm;

emission: 520 nm) induced by various concentrations of the compounds were recorded in each well. Experiments were performed in triplicates and the averaged data (as well as SEM) were used in the calculations.

Statistical analysis

Data were analyzed by IBM SPSS Statistics 19 (SPSS Inc.) software, using Student's two tailed two samples *t*-test (paired comparisons) or one-way ANOVA with Bonferroni's and Dunnett's post hoc probes (multiple comparisons) and $P<0.05$ values were regarded as significant differences. Homogeneity of variances were analyzed by Levene's test. If Levene's test indicated inhomogeneity of variances, Games-Howel test was used instead of Bonferroni. Graphs were plotted by using Origin Pro Plus 6.0 software (Microcal).

Study approval

This study was approved by the Institutional Research Ethics Committee (University of Lübeck) and adhered to the Declaration of Helsinki Principle guidelines. Study subjects provided informed consent prior to their participation.

2. Supplemental Tables

Supplemental Table 1. *List of genes that were significantly down-regulated (3 independent treatments, at least 2-fold equi-directional changes in all cases, P<0.05) by CBD treatment of human SZ95 sebocytes*

Gene Name	Description	Average Fold Change	Note
MID1	Homo sapiens midline 1 (Opitz/BBB syndrome) (MID1), transcript variant 3, mRNA [NM_033290]	0.144583754	
SLC39A10	Homo sapiens solute carrier family 39 (zinc transporter), member 10 (SLC39A10), mRNA [NM_020342]	0.179378308	Same effect was shown in BV-2 microglia cells; SLC39A10 is involved in Zn^{2+}-efflux (81).
ENST00000380787	Unknown	0.218302567	
NAT1	Homo sapiens N-acetyltransferase 1 (arylamine N-acetyltransferase) (NAT1), mRNA [NM_000662]	0.220518435	
CD24	Homo sapiens CD24 signal transducer mRNA, complete cds and 3' region. [L33930]	0.244703822	
A_32_P82293	Unknown	0.276372603	
ARHGAP24	Homo sapiens cDNA FLJ27066 fis, clone SPL01327. [AK130576]	0.286928365	
DAAM1	Homo sapiens disheveled associated activator of morphogenesis 1 (DAAM1), mRNA [NM_014992]	0.288870651	It is thought to function as a scaffolding protein for the Wnt-induced assembly of a disheveled (Dvl)-Rho complex (82).
OPN3	Homo sapiens opsin 3 (encephalopsin, panopsin) (OPN3), transcript variant 1, mRNA [NM_014322]	0.294213681	
LAMB1	Homo sapiens laminin, beta 1 (LAMB1), mRNA [NM_002291]	0.295427431	
NTN4	Homo sapiens netrin 4 (NTN4), mRNA [NM_021229]	0.297136326	It promotes cellular proliferation (83).
BF508144	UI-H-BI4-apz-e-08-0-UI.s1 NCI_CGAP_Sub8 Homo sapiens cDNA clone IMAGE:3089007 3', mRNA sequence [BF508144]	0.298223395	
PRSS23	Homo sapiens protease, serine, 23 (PRSS23), mRNA [NM_007173]	0.301106646	
STEAP4	Homo sapiens STEAP family member 4 (STEAP4), mRNA [NM_024636]	0.303239595	It is thought to be involved in adipocyte differentiation (84).
SPTLC2L	Homo sapiens cDNA FLJ90790 fis, clone THYRO1001529, moderately similar to Serine palmitoyltransferase 2 (EC 2.3.1.50). [AK075271]	0.304280871	
FOXA1	Homo sapiens forkhead box A1 (FOXA1), mRNA [NM_004496]	0.304794447	It is a mesenchymal differentiation marker (85).

LXN	Homo sapiens latexin (LXN), mRNA [NM_020169]	0.309134992	
NRIP1	Homo sapiens nuclear receptor interacting protein 1 (NRIP1), mRNA [NM_003489]	0.309212846	Essential for triglyceride storage in adipose tissue (46).
TLR1	Homo sapiens toll-like receptor 1 (TLR1), mRNA [NM_003263]	0.312672783	Role in innate immunity (86).
ENST00000353442	Unknown	0.314827882	
MAP4K3	Homo sapiens mitogen-activated protein kinase kinase kinase kinase 3 (MAP4K3), mRNA [NM_003618]	0.325163457	It plays a role in the activation of mTORC1 (87), which is thought to have “pro-acne” effects (43).
TRAM1	Homo sapiens translocation associated membrane protein 1 (TRAM1), mRNA [NM_014294]	0.327653171	
THC2386010	Unknown	0.331284758	
TPMT	Homo sapiens thiopurine S-methyltransferase (TPMT), mRNA [NM_000367]	0.332831935	
LMO7	Homo sapiens LIM domain 7 (LMO7), mRNA [NM_005358]	0.334474202	
THC2367825	Q9N3X9 (Q9N3X9) Collagen protein 115, partial (5%) [THC2367825]	0.335682775	
ENST00000367385	Homo sapiens mRNA; cDNA DKFZp586G2222 (from clone DKFZp586G2222). [AL080111]	0.336935039	
THC2279364	ALU8_HUMAN (P39195) Alu subfamily SX sequence contamination warning entry, partial (4%) [THC2279364]	0.337174074	
AV698092	AV698092 GKC Homo sapiens cDNA clone GKCGUA09 5', mRNA sequence [AV698092]	0.344919878	
AF086216	Homo sapiens full length insert cDNA clone ZC65B11. [AF086216]	0.344946688	
ZNF702	Homo sapiens cDNA FLJ12985 fis, clone NT2RP3000050, moderately similar to ZINC FINGER PROTEIN 91. [AK023047]	0.349667263	
EFEMP1	Homo sapiens EGF-containing fibulin-like extracellular matrix protein 1 (EFEMP1), transcript variant 1, mRNA [NM_004105]	0.350370379	
LOC649791	PREDICTED: Homo sapiens similar to general transcription factor II, i isoform 1, transcript variant 4 (LOC649791), mRNA [XM_943120]	0.351190156	
KIAA0101	Homo sapiens KIAA0101 (KIAA0101), transcript variant 1, mRNA [NM_014736]	0.353153053	
POT1	Homo sapiens POT1 protection of telomeres 1 homolog (S. pombe) (POT1), mRNA [NM_015450]	0.35484116	
AF113674	Homo sapiens clone FLB1727 PRO0398 mRNA, complete cds. [AF113674]	0.359119921	

RP4-747L4.3	Homo sapiens hypothetical protein MGC12538, mRNA (cDNA clone MGC:12538 IMAGE:3839075), complete cds. [BC007072]	0.359262384	
KLF5	Homo sapiens Kruppel-like factor 5 (intestinal) (KLF5), mRNA [NM_001730]	0.360155512	It is pro-proliferative in epithelial cells (88).
ENST00000297145	Homo sapiens PNAS-12 mRNA, partial sequence. [AF274937]	0.361030612	
C6orf211	Homo sapiens chromosome 6 open reading frame 211 (C6orf211), mRNA [NM_024573]	0.365046799	
AK056245	Homo sapiens cDNA FLJ31683 fis, clone NT2RI2005353. [AK056245]	0.366099279	
PHKB	Homo sapiens phosphorylase kinase, beta (PHKB), transcript variant 1, mRNA [NM_000293]	0.36678392	
BF509482	UI-H-BI4-aoz-b-08-0-UI.s1 NCI_CGAP_Sub8 Homo sapiens cDNA clone IMAGE:3086535 3', mRNA sequence [BF509482]	0.370735322	
AL832758	Homo sapiens mRNA; cDNA DKFZp686C0927 (from clone DKFZp686C0927). [AL832758]	0.371776581	
ENST00000373218	Homo sapiens mRNA; cDNA DKFZp762K067 (from clone DKFZp762K067). [CR627373]	0.372494994	
PDE8A	Homo sapiens phosphodiesterase 8A (PDE8A), transcript variant 5, mRNA [NM_173457]	0.377251072	
FAM62B	Homo sapiens family with sequence similarity 62 (C2 domain containing) member B (FAM62B), mRNA [NM_020728]	0.378298525	
SCEL	Homo sapiens sciellin (SCEL), transcript variant 2, mRNA [NM_144777]	0.382019937	
NXT2	Homo sapiens nuclear transport factor 2-like export factor 2 (NXT2), mRNA [NM_018698]	0.382153336	
ARHGEF3	Homo sapiens Rho guanine nucleotide exchange factor (GEF) 3 (ARHGEF3), mRNA [NM_019555]	0.382355051	
THC2314901	BC004536 carnitine deficiency-associated gene expressed in ventricle 1 {Homo sapiens;} , partial (7%) [THC2314901]	0.382570549	
AL133577	Homo sapiens mRNA; cDNA DKFZp434G0972 (from clone DKFZp434G0972). [AL133577]	0.383756041	
ENST00000367142	Q62VJ0 (Q62VJ0) Small peptidoglycan-associated lipoprotein, partial (13%) [THC2301029]	0.385407708	
DEPDC7	Homo sapiens DEP domain containing 7 (DEPDC7), mRNA [NM_139160]	0.386647666	
ZNF426	Homo sapiens zinc finger protein 426 (ZNF426), mRNA [NM_024106]	0.387439082	

PCYOX1	Homo sapiens prenylcysteine oxidase 1 (PCYOX1), mRNA [NM_016297]	0.387560426	
SFRP1	Homo sapiens secreted frizzled-related protein 1 (SFRP1), mRNA [NM_003012]	0.392834472	It inhibits WNT-signaling (89). WNT is an inhibitor of sebaceous differentiation (90).
GTF2I	Homo sapiens general transcription factor II, i (GTF2I), transcript variant 1, mRNA [NM_032999]	0.394530829	
ADNP	Homo sapiens activity-dependent neuroprotector (ADNP), transcript variant 1, mRNA [NM_015339]	0.399327536	
SVIL	Homo sapiens supervillin (SVIL), transcript variant 2, mRNA [NM_021738]	0.400968078	
BG163514	602338531F1 NIH_MGC_89 Homo sapiens cDNA clone IMAGE:4446534 5', mRNA sequence [BG163514]	0.403181706	
SLFN12	Homo sapiens schlafen family member 12 (SLFN12), mRNA [NM_018042]	0.408594415	
UBE1C	Homo sapiens ubiquitin-activating enzyme E1C (UBA3 homolog, yeast) (UBE1C), transcript variant 1, mRNA [NM_003968]	0.409550306	
CENPI	Homo sapiens centromere protein I (CENPI), mRNA [NM_006733]	0.416365112	
FLJ22624	Homo sapiens FLJ22624 protein (FLJ22624), mRNA [NM_024808]	0.41913823	
HMGN3	Homo sapiens high mobility group nucleosomal binding domain 3 (HMGN3), transcript variant 2, mRNA [NM_138730]	0.424725991	
BTBD1	Homo sapiens BTB (POZ) domain containing 1 (BTBD1), transcript variant 1, mRNA [NM_025238]	0.42599776	
ENST00000367612	Homo sapiens cDNA FLJ11174 fis, clone PLACE1007367. [AK002036]	0.432484207	
FAM96A	Homo sapiens family with sequence similarity 96, member A (FAM96A), transcript variant 1, mRNA [NM_032231]	0.438190306	
ENST00000366751	Homo sapiens mRNA full length insert cDNA clone EUROIMAGE 2068962. [AJ420589]	0.438266468	
FRK	Homo sapiens fyn-related kinase (FRK), mRNA [NM_002031]	0.444706282	
NCOA7	Homo sapiens nuclear receptor coactivator 7 (NCOA7), mRNA [NM_181782]	0.445200315	
TCEAL1	Homo sapiens transcription elongation factor A (SII)-like 1 (TCEAL1), transcript variant 3, mRNA [NM_001006640]	0.447935262	
SERPINB9	Homo sapiens serpin peptidase inhibitor, clade B (ovalbumin), member 9 (SERPINB9), mRNA [NM_004155]	0.451637699	

CCBE1	Homo sapiens collagen and calcium binding EGF domains 1 (CCBE1), mRNA [NM_133459]	0.454814193	
RBM7	Homo sapiens RNA binding motif protein 7 (RBM7), mRNA [NM_016090]	0.462986923	
MKI67	Homo sapiens antigen identified by monoclonal antibody Ki-67 (MKI67), mRNA [NM_002417]	0.474182345	Proliferation marker (91).
THC2342537	ALU1_HUMAN (P39188) Alu subfamily J sequence contamination warning entry, partial (5%) [THC2342537]	0.475837891	
GPIAP1	Homo sapiens GPI-anchored membrane protein 1 (GPIAP1), transcript variant 2, mRNA [NM_203364]	0.490956422	
FLJ20273	Homo sapiens RNA-binding protein (FLJ20273), mRNA [NM_019027]	0.494577039	

Supplemental Table 2. *List of genes that were significantly (3 independent treatments, at least 2-fold equi-directional changes in all cases, P<0.05) up-regulated by CBD treatment of human SZ95 sebocytes*

GeneName	Description	Average Fold Change	Note
LOC150383	Homo sapiens similar to RIKEN cDNA 2210021J22, transcript variant 1, mRNA (cDNA clone MGC:87534 IMAGE:30338205), complete cds. [BC067871]	2.023020498	
CICE	Homo sapiens cell death-inducing CIDE-like effector pseudogene (CICE) on chromosome 3 [NR_002786]	2.028682357	
LOC145853	PREDICTED: Homo sapiens hypothetical LOC145853 (LOC145853), mRNA [XM_096885]	2.050746331	
THC2296299	Unknown	2.052834221	
AA532655	nj17d09.s1 NCI_CGAP_Pr22 Homo sapiens cDNA clone IMAGE:986609 3', mRNA sequence [AA532655]	2.100324768	
SH2D5	Homo sapiens cDNA FLJ42879 fis, clone BRHIP3001283. [AK124869]	2.10832994	
CDH4	Homo sapiens cadherin 4, type 1, R-cadherin (retinal) (CDH4), mRNA [NM_001794]	2.109778874	
ENST00000269290	Homo sapiens HSPC254 mRNA, partial cds. [AF161372]	2.114503823	
ATF4	Homo sapiens activating transcription factor 4 (tax-responsive enhancer element B67) (ATF4), transcript variant 1, mRNA [NM_001675]	2.138734073	It is a down-stream molecule of TRIB3-signaling (66).
GOT1	Homo sapiens glutamic-oxaloacetic transaminase 1, soluble (aspartate aminotransferase 1) (GOT1), mRNA [NM_002079]	2.1476287	
C6orf1	Homo sapiens chromosome 6 open reading frame 1 (C6orf1), transcript variant 1, mRNA [NM_178508]	2.188775606	
SLC1A4	Homo sapiens solute carrier family 1 (glutamate/neutral amino acid transporter), member 4 (SLC1A4), mRNA [NM_003038]	2.191168404	
ZNF598	Homo sapiens zinc finger protein 598 (ZNF598), mRNA [NM_178167]	2.221106279	
ABCB6	Homo sapiens ATP-binding cassette, sub-family B (MDR/TAP), member 6 (ABCB6), nuclear gene encoding mitochondrial protein, mRNA [NM_005689]	2.238983054	
FUT1	Homo sapiens fucosyltransferase 1 (galactoside 2-alpha-L-fucosyltransferase, H blood group) (FUT1), mRNA [NM_000148]	2.24477072	

ST6GALNAC4	Homo sapiens ST6 (alpha-N-acetyl-neuraminyl-2,3-beta-galactosyl-1,3)-N-acetylgalactosaminide alpha-2,6-sialyltransferase 4 (ST6GALNAC4), transcript variant 1, mRNA [NM_175039]	2.249856903	
WARS	Homo sapiens tryptophanyl-tRNA synthetase (WARS), transcript variant 1, mRNA [NM_004184]	2.262522437	
MYBBP1A	Homo sapiens MYB binding protein (P160) 1a (MYBBP1A), mRNA [NM_014520]	2.285565522	It is a repressor of NF-κB (92).
AK123450	Homo sapiens cDNA FLJ41456 fis, clone BRSTN2012320. [AK123450]	2.291105966	
LOC645427	Homo sapiens cDNA FLJ37088 fis, clone BRACE2017124. [AK094407]	2.299131401	
A_32_P146871	Unknown	2.325869291	
UBIAD1	Homo sapiens UbiA prenyltransferase domain containing 1 (UBIAD1), mRNA [NM_013319]	2.326335569	
TIGA1	Homo sapiens TIGA1 (TIGA1), mRNA [NM_053000]	2.332263761	It inhibits proliferation via maintaining G_0 phase (93).
NAGS	Homo sapiens N-acetylglutamate synthase (NAGS), mRNA [NM_153006]	2.354736066	
SLC3A2	Homo sapiens solute carrier family 3 (activators of dibasic and neutral amino acid transport), member 2 (SLC3A2), transcript variant 3, mRNA [NM_002394]	2.372841331	
SARS	Homo sapiens seryl-tRNA synthetase (SARS), mRNA [NM_006513]	2.3754084	
ZFAND2A	Homo sapiens zinc finger, AN1-type domain 2A (ZFAND2A), mRNA [NM_182491]	2.395515359	
AK129849	Homo sapiens cDNA FLJ26339 fis, clone HRT02975. [AK129849]	2.396346358	
PHGDH	Homo sapiens phosphoglycerate dehydrogenase (PHGDH), mRNA [NM_006623]	2.401009252	
ETV4	Homo sapiens ets variant gene 4 (E1A enhancer binding protein, E1AF) (ETV4), mRNA [NM_001986]	2.415031911	
AW275876	xq40c08.x1 NCI_CGAP_Lu28 Homo sapiens cDNA clone IMAGE:2753102 3' similar to gb:X57352 INTERFERON-INDUCIBLE PROTEIN 1-8U (HUMAN);, mRNA sequence [AW275876]	2.41597705	
GPT2	Homo sapiens glutamic pyruvate transaminase (alanine aminotransferase) 2 (GPT2), mRNA [NM_133443]	2.418307046	
LARP6	Homo sapiens La ribonucleoprotein domain family, member 6 (LARP6), transcript variant 1, mRNA [NM_018357]	2.424631034	

THC2370432	AL547890 AL547890 Homo sapiens PLACENTA COT 25-NORMALIZED Homo sapiens cDNA clone CS0DI033YB09 5-PRIME, mRNA sequence [AL547890]	2.436811494	
A_24_P204414	Unknown	2.442940076	
CHAC1	Homo sapiens ChaC, cation transport regulator-like 1 (E. coli) (CHAC1), mRNA [NM_024111]	2.449755082	Down-stream of ATF4 (67).
BEX2	Homo sapiens brain expressed X-linked 2 (BEX2), mRNA [NM_032621]	2.517811045	
IGSF4B	Homo sapiens immunoglobulin superfamily, member 4B (IGSF4B), mRNA [NM_021189]	2.535371171	
SDSL	Homo sapiens serine dehydratase-like (SDSL), mRNA [NM_138432]	2.538715595	
AK026372	Homo sapiens cDNA: FLJ22719 fis, clone HSI14307. [AK026372]	2.555616463	
C3AR1	Homo sapiens complement component 3a receptor 1 (C3AR1), mRNA [NM_004054]	2.570060685	
HERPUD1	Homo sapiens homocysteine-inducible, endoplasmic reticulum stress-inducible, ubiquitin-like domain member 1 (HERPUD1), transcript variant 1, mRNA [NM_014685]	2.571099986	
BU733098	BU733098 UI-E-CI1-afo-h-12-0-UI.s1 UI-E-CI1 Homo sapiens cDNA clone UI-E-CI1-afo-h-12-0-UI 3', mRNA sequence [BU733098]	2.637830353	
EXOSC5	Homo sapiens exosome component 5 (EXOSC5), mRNA [NM_020158]	2.692247637	
KCNG1	Homo sapiens potassium voltage-gated channel, subfamily G, member 1 (KCNG1), transcript variant 2, mRNA [NM_172318]	2.703684623	
SH2D2A	Homo sapiens SH2 domain protein 2A (SH2D2A), mRNA [NM_003975]	2.75980934	
AL581249	AL581249 AL581249 Homo sapiens B CELLS (RAMOS CELL LINE) Homo sapiens cDNA clone CS0DG001YB03 3-PRIME, mRNA sequence [AL581249]	2.775465209	
THC2269172	Unknown	2.927166352	
HIST2H2AA3	Homo sapiens histone 2, H2aa3 (HIST2H2AA3), mRNA [NM_003516]	2.938759743	
YARS	Homo sapiens tyrosyl-tRNA synthetase (YARS), mRNA [NM_003680]	2.94243008	
THC2268341	HSU18930 MHC class I antigen HLA-A2 {Homo sapiens;} , partial (24%) [THC2268341]	2.965358743	
SLC1A5	Homo sapiens solute carrier family 1 (neutral amino acid transporter), member 5 (SLC1A5), mRNA [NM_005628]	2.99104015	
CAMP	Homo sapiens cathelicidin antimicrobial peptide (CAMP), mRNA [NM_004345]	3.005000572	A key anti-microbial peptide (49).

ARHGAP9	Homo sapiens Rho GTPase activating protein 9 (ARHGAP9), mRNA [NM_032496]	3.051559194	It inhibits ERK2 (46).
RHEBL1	Homo sapiens Ras homolog enriched in brain like 1 (RHEBL1), mRNA [NM_144593]	3.093509903	
ENST00000377492	Homo sapiens cDNA clone IMAGE:4826036, containing frame-shift errors. [BC032035]	3.132671285	
CTH	Homo sapiens cystathionase (cystathionine gamma-lyase) (CTH), transcript variant 1, mRNA [NM_001902]	3.14257467	
BF689038	BF689038 602185294T1 NIH_MGC_43 Homo sapiens cDNA clone IMAGE:4299791 3', mRNA sequence [BF689038]	3.20570321	
ASNS	Homo sapiens asparagine synthetase (ASNS), transcript variant 2, mRNA [NM_001673]	3.286716977	It is a down-stream target of TRIB3-ATF4 axis (66).
SLC5A12	Homo sapiens solute carrier family 5 (sodium/glucose cotransporter), member 12 (SLC5A12), transcript variant 2, mRNA [NM_178498]	3.304062131	
THC2375394	Unknown	3.3240169	
TRIB3	Homo sapiens tribbles homolog 3 (Drosophila) (TRIB3), mRNA [NM_021158]	3.393634165	Negative regulator of NF-κB (50), it suppresses adipocyte differentiation (63).
LOC645733	PREDICTED: Homo sapiens hypothetical LOC389025 (LOC389025), mRNA [XM_374004]	3.397325086	
IL29	Homo sapiens interleukin 29 (interferon, lambda 1) (IL29), mRNA [NM_172140]	3.503097918	
EFCBP2	Homo sapiens EF-hand calcium binding protein 2 (EFCBP2), mRNA [NM_019065]	3.509125629	
GDF15	Homo sapiens growth differentiation factor 15 (GDF15), mRNA [NM_004864]	3.593744623	GDF15 overexpressing mice are lean and show reduced inflammatory responses (94).
KCTD15	Homo sapiens potassium channel tetramerisation domain containing 15 (KCTD15), mRNA [NM_024076]	3.651733545	
THC2340759	Unknown	3.871258178	
PCK2	Homo sapiens phosphoenolpyruvate carboxykinase 2 (mitochondrial) (PCK2), nuclear gene encoding mitochondrial protein, transcript variant 1, mRNA [NM_004563]	3.88005262	
STC2	Homo sapiens stanniocalcin 2 (STC2), mRNA [NM_003714]	3.951302081	
DDIT3	Homo sapiens DNA-damage-inducible transcript 3 (DDIT3), mRNA [NM_004083]	6.59893248	It is a down-stream target of TRIB3-ATF4 axis (66).

THC2363646	AJHYNG asparagine synthase (glutamine-hydrolysing) [similarity] - golden hamster {Mesocricetus auratus;} , partial (17%) [THC2363646]	7.040593326	

3. Supplemental Figures

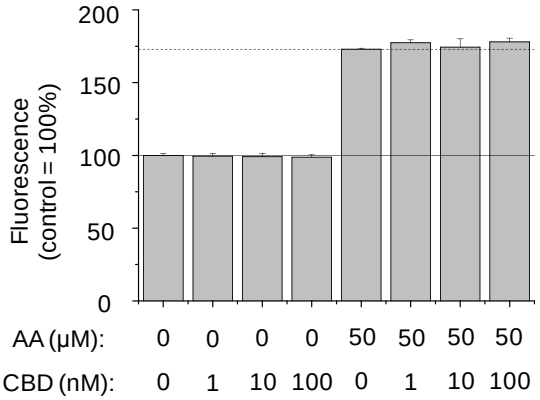

Supplemental Figure 1. *Low concentrations of CBD exert no effect on either basal or AA-induced lipid synthesis of human sebocytes*
Neutral lipid synthesis (Nile Red staining). Cells were treated by arachidonic acid (AA) and/or cannabidiol (CBD) for 48 hrs. Data are expressed as mean±SEM of four independent determinations as the percentage of the vehicle control (100%, solid line). One additional experiment yielded similar results.

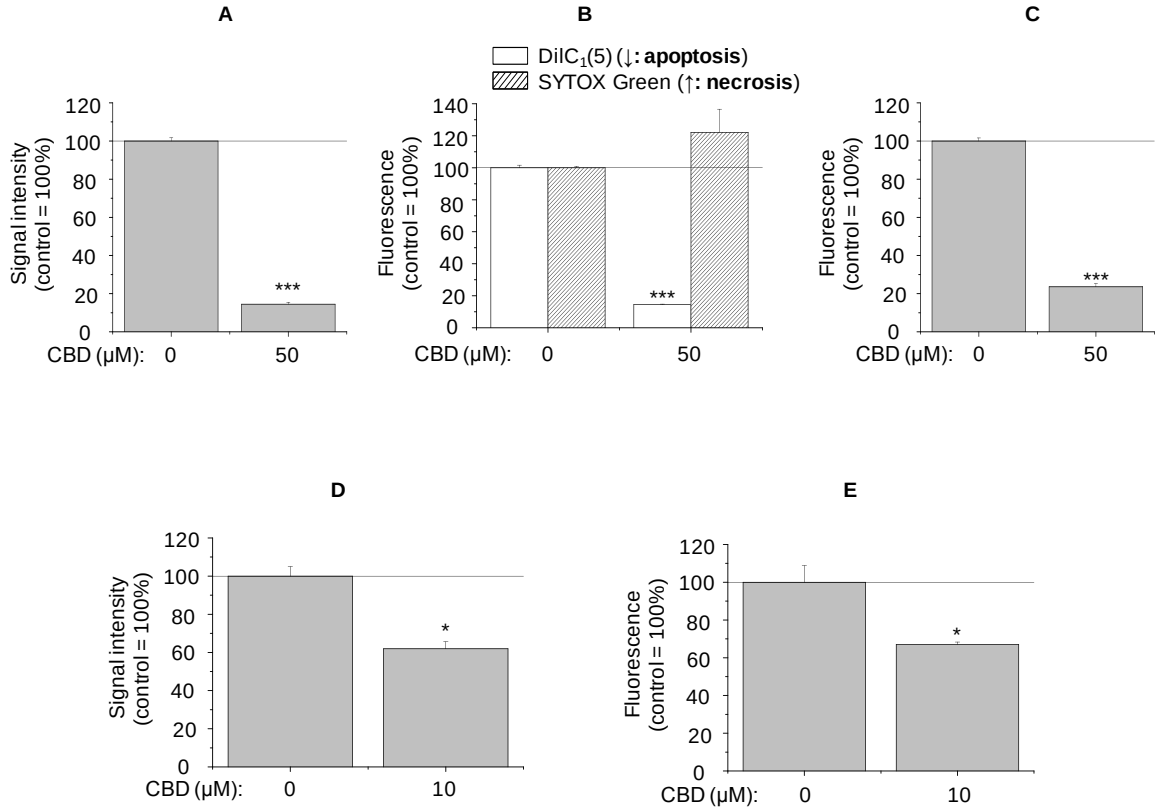

Supplemental Figure 2. *High concentrations or long-term applications of CBD decrease human sebocyte viability and lipid production*
(**A**) MTT-assay. Viability of sebocytes following 48-hr treatments. CBD: cannabidiol. ****P*<0.001. (**B**) Cell death ($DilC_1(5)$-SYTOX Green double labeling) assays (after 24-hr treatments). (**C**) Neutral lipid synthesis (Nile Red staining). Cells were treated by CBD for 48 hrs. ****P*<0.001. (**D**) MTT-assay. Viability of sebocytes following 6-day treatments. **P*<0.05. (**E**) Neutral lipid synthesis (Nile Red staining). Cells were treated by CBD for 6 days. **P*<0.05. (**A**, **B, C, D, E**) Results are expressed in the percentage of the vehicle control (100%, solid line) as mean±SEM of four independent determinations. One additional experiment yielded similar results.

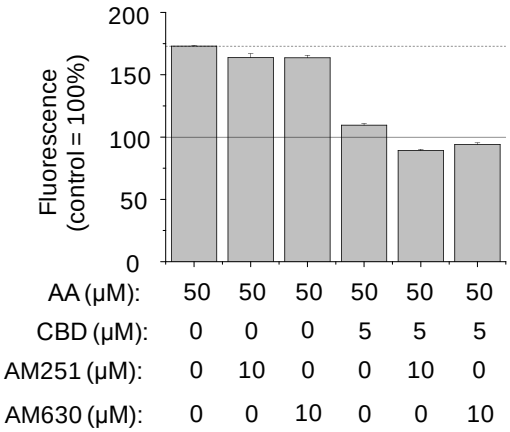

Supplemental Figure 3. *Effects of CBD are not mediated by CB1 or CB2 receptors*

Neutral lipid synthesis (Nile Red staining). Cells were treated with arachidonic acid (AA), cannabidiol (CBD), AM251 (CB1 receptor antagonist), AM630 (CB2 receptor antagonist) or combinations for 24 hrs. Data are expressed as mean±SEM of four independent determinations as the percentage of the vehicle control (100%, solid line). One additional experiment yielded similar results.

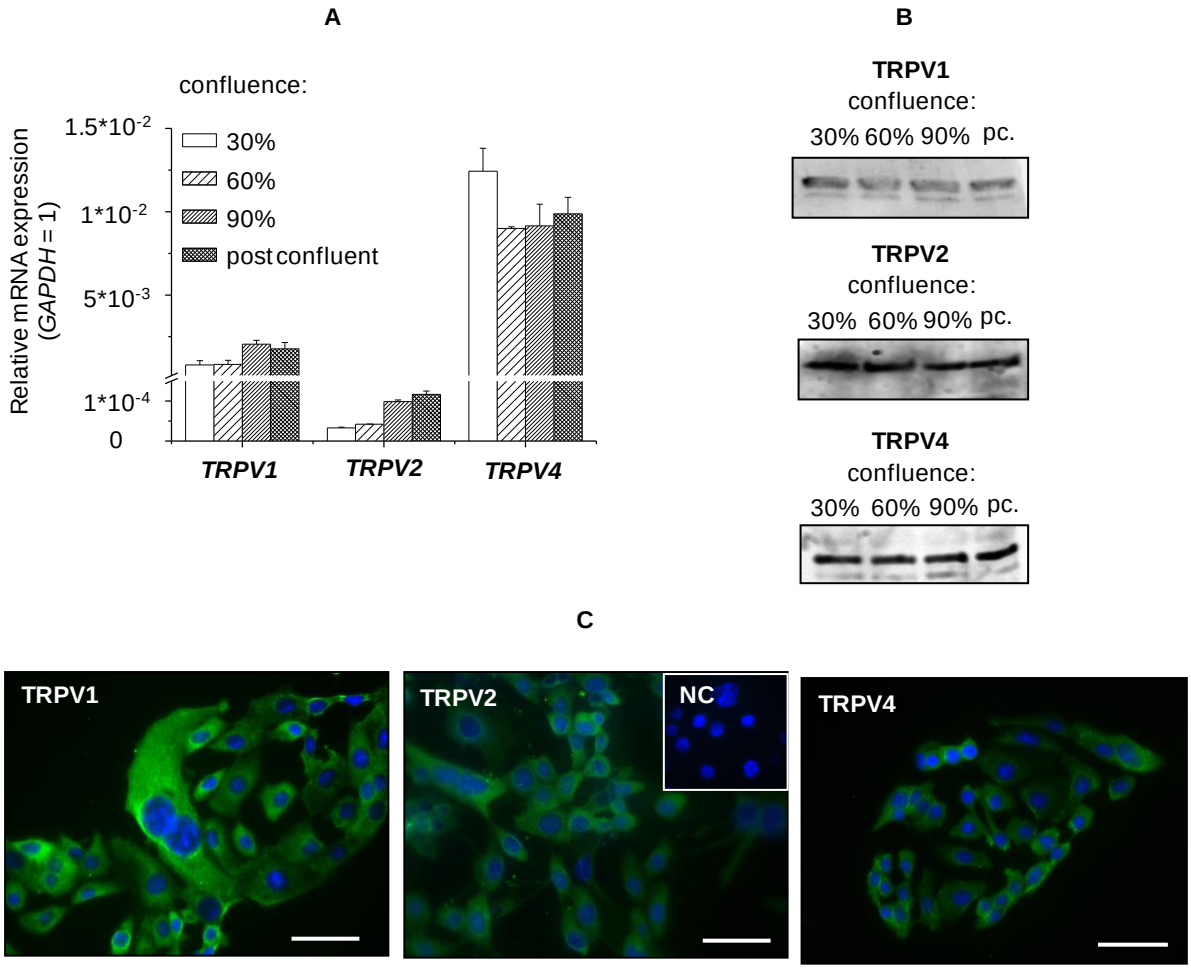

Supplemental Figure 4. *Human SZ95 sebocytes express certain TRP channels*

(**A**) Quantitative "real time" PCR on SZ95 sebocyte samples harvested at different confluences. Data of *TRPV1*, *TRPV2* and *TRPV4* mRNA expressions were normalized to the level of glyceraldehyde-3-phosphate dehydrogenase (*GAPDH*) of the same sample, and are expressed as mean±SEM of three independent determinations. Two additional experiments yielded similar results. (**B**) Western blot analysis of lysates of SZ95 sebocytes (pc: post-confluent culture). (**C**) Immunocytochemistry. TRPV1, TRPV2 and TRPV4-specific immunreactivity was determined by immunofluorescence labeling (Alexa-Fluor®-488, green fluorescence) in SZ95 sebocytes. Nuclei were counterstained by DAPI (blue fluorescence). NC: negative control. Scale bars: 20 μm.

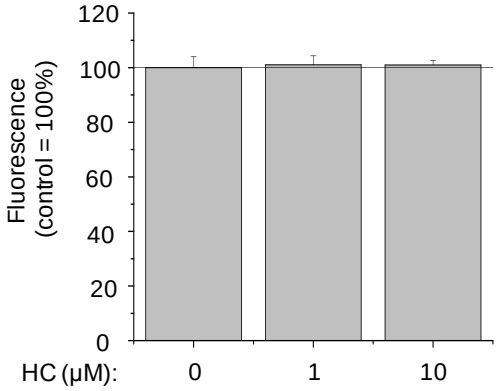

Supplemental Figure 5. *Antagonism of TRPV4 exerts no effect on basal lipid synthesis of human sebocytes*

Neutral lipid synthesis (Nile Red staining). Cells were treated with HC067047 (HC) for 48 hrs. Data are expressed as mean±SEM of four independent determinations as the percentage of the vehicle control (100%, solid line). One additional experiment yielded similar results.

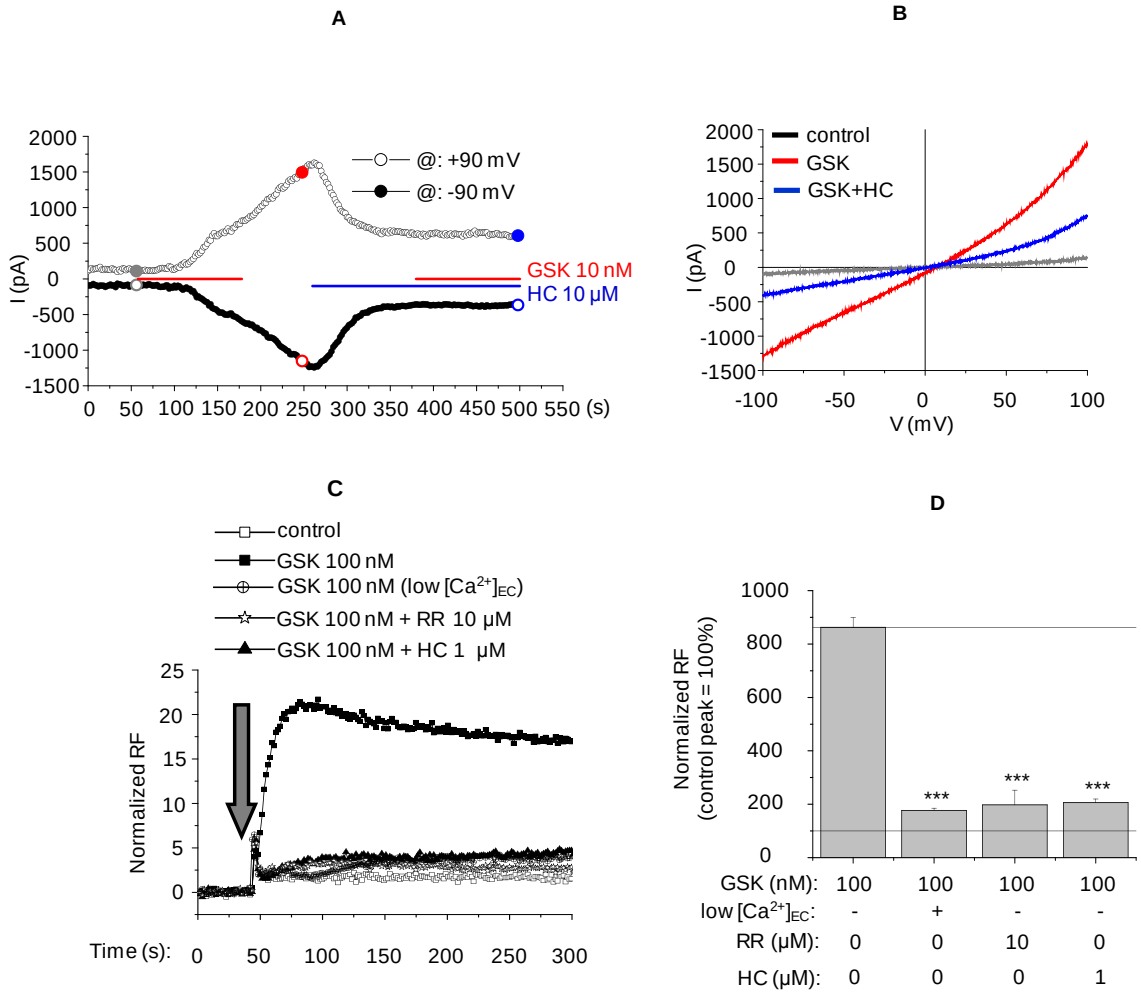

Supplemental Figure 6. *TRPV4 is functionally expressed by human sebocytes*

(**A**) Time course of whole current at -90 and +90 mV in SZ95 sebocytes treated by 10 nM GSK1016790A (GSK) and 10 µM HC067047 (HC), as indicated in the figure. (**B**) Current-voltage traces at different time points as indicated in panel **A**. (**C**) Fluorescent Ca^{2+}-imaging. Compounds were applied as indicated by the arrow. Fluorescence (measured in relative fluorescence units, RF) was normalized to the baseline. GSK: GSK1016790A, HC: HC067047, RR: ruthenium red, low $[Ca^{2+}]_{EC}$: nominally Ca^{2+}-free Hank's solution. (**D**) Statistical analysis of the Ca^{2+}-imaging data shown in panel **C**. Measured peak values were expressed in the percentage of the peak value of the control (100%, solid line) as mean±SEM of 3 independent determinations. Two additional experiments yielded similar results. ***P<0.001 compared to the GSK-treated group.

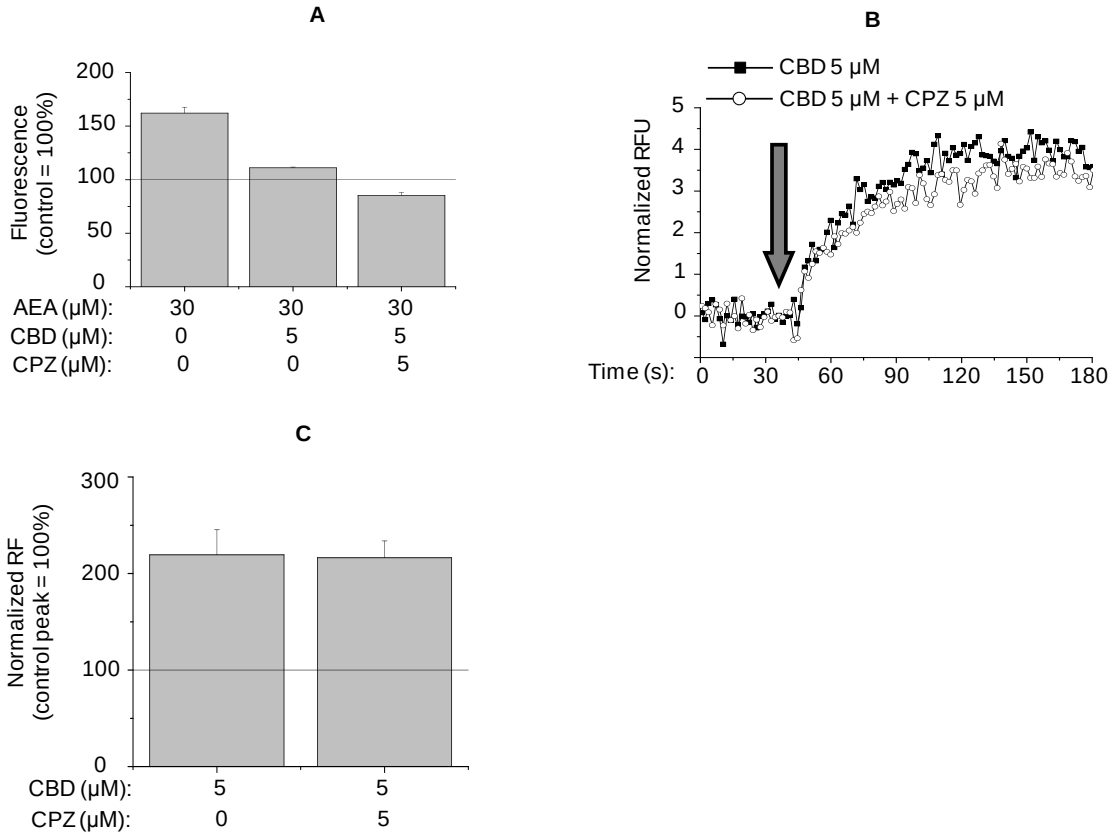

Supplemental Figure 7. *Effects of CBD on human sebocytes are not mediated by TRPV1*

(**A**) Neutral lipid synthesis (Nile Red staining). Cells were treated by anandamide (AEA), cannabidiol (CBD), capsazepine (CPZ), or combination for 24 hrs. Data are expressed as mean±SEM of four independent determinations as the percentage of the vehicle control (100%, solid line). Two additional experiments yielded similar results. (**B**) Fluorescent Ca^{2+}-imaging. Compounds were applied as indicated by the arrow. Fluorescence (measured in relative fluorescence units, RF) was normalized to the baseline (100%). (**C**) Statistical analysis of the Ca^{2+}-imaging data. Measured peak values were expressed in the percentage of the peak value of the control (100%, solid line) as mean±SEM of 3 independent determinations. Two additional experiments yielded similar results.

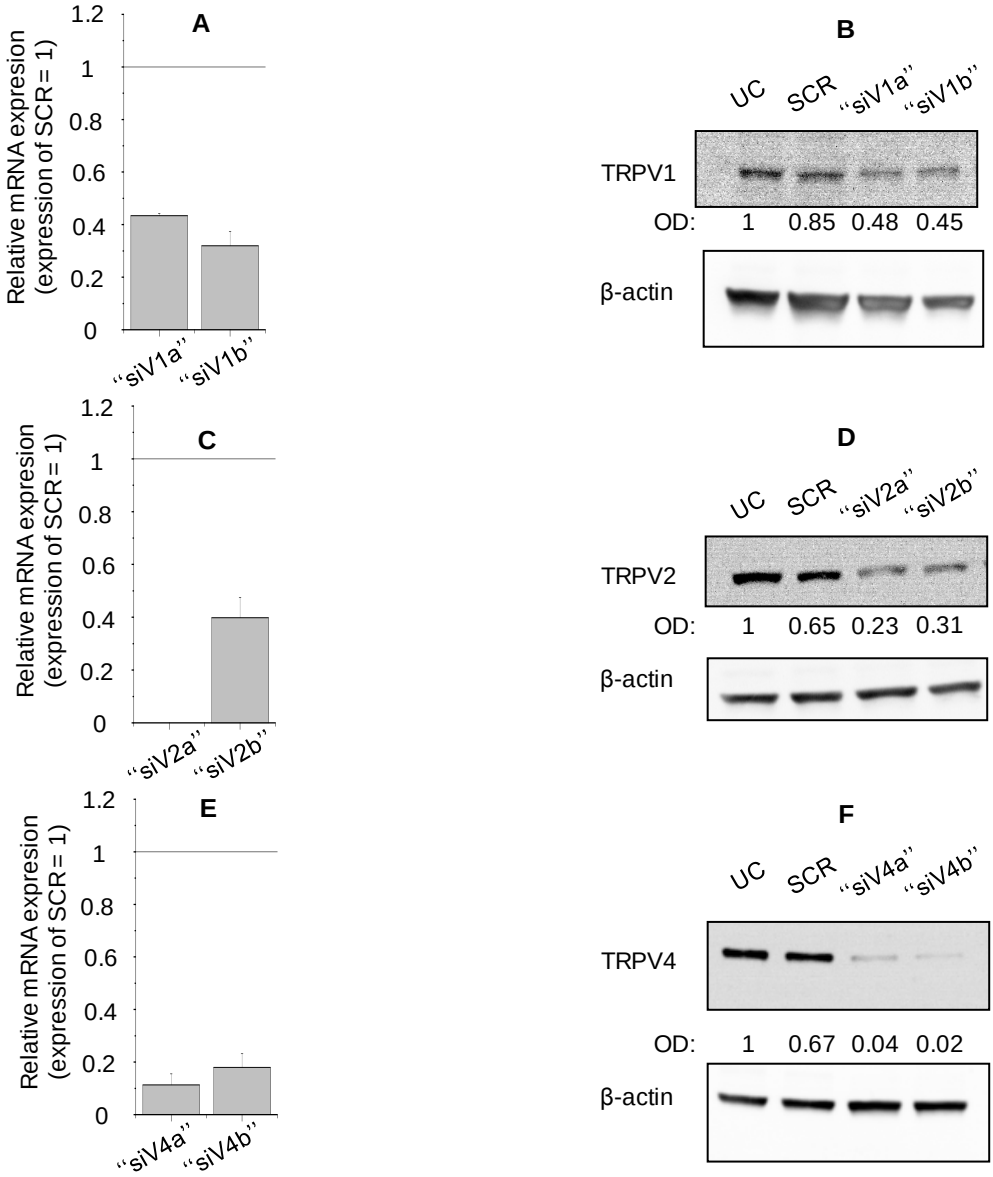

Supplemental Figure 8. *Evaluation of efficacy of selective gene silencing of TRPV channels*

(**A**, **C** and **E**) *TRPV1*, *TRPV2* and *TRPV4* mRNA expressions two days after their selective gene silencing. Data are presented by using ΔΔCT method regarding glyceraldehyde-3-phosphate dehydrogenase (*GAPDH*) or peptidil-prolyl isomerase A (*PPIA*) normalized TRPV mRNA expression of the appropriate scrambled (SCR) control as 1 (solid line). Data are expressed as mean±SD of three independent determinations. (**B**, **D** and **F**) Western blot analyses of lysates of un-transfected (UC), non-sense RNA transfected (SCR: scrambled control), and TRPV1-, TRPV2- and TRPV4-silenced SZ95 sebocytes, respectively, three days after the transfection. OD: β-actin-normalized optical density of the corresponding bands. "siV1a", "siV1b", "siV2a", "siV2b", "siV4a" and "siV4b" mark different siRNA constructs against TRPV1, TRPV2 and TRPV4, respectively.

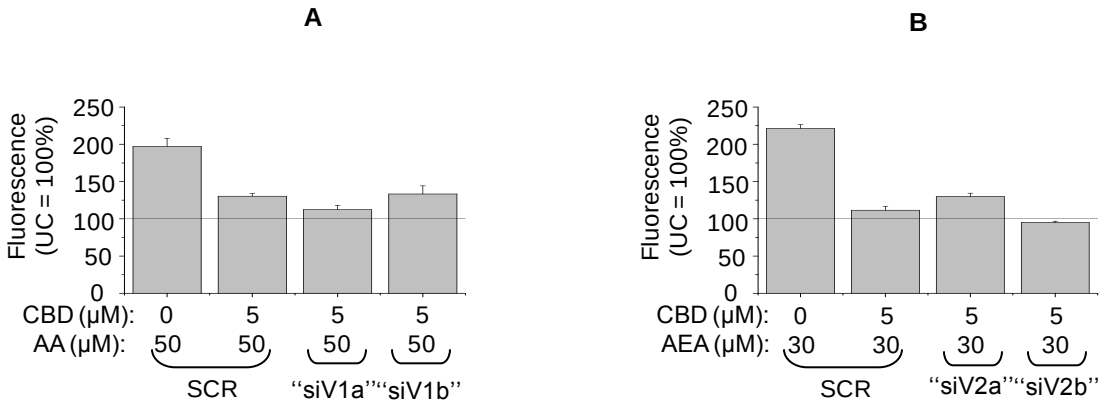

Supplemental Figure 9. *Neither TRPV1, nor TRPV2 mediates the lipostatic effects of CBD*

(**A** and **B**) Neutral lipid synthesis (Nile Red staining) following selective gene silencing of TRPV1 (**A**) or TRPV2 (**B**) channels (24-hr treatments, started at day 3 after transfection). Data are expressed as mean±SEM of four independent determinations as the percentage of the untransfected vehicle control (100%, solid line). Two additional experiments yielded similar results. SCR: scrambled control. In panel **A** "siV1a" and "siV1b" mark different siRNA constructs against TRPV1, whereas in panel **B** "siV2a" and "siV2b" mark two different siRNA constructs against TRPV2. AA: arachidonic acid, AEA: anandamide, UC: untransfected vehicle control.

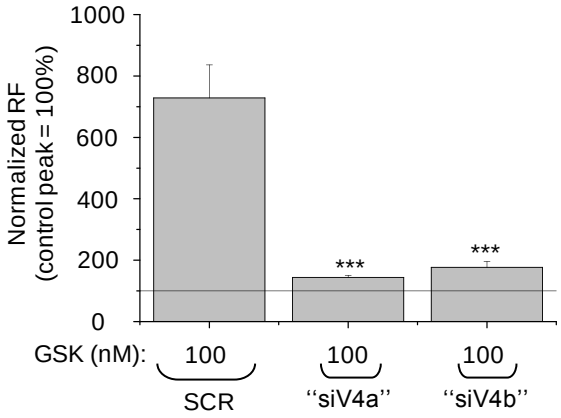

Supplemental Figure 10. *Silencing of TRPV4 effectively abrogates its functionality*

Statistical analysis of fluorescent Ca^{2+}-imaging data, obtained after GSK1016790A (GSK) challenges on TRPV4 "silenced" SZ95 sebocytes. Measured peak values were expressed in the percentage of the peak value of the control (100%, solid line) as mean±SEM of 8 independent determinations. One additional experiment yielded similar results. "siV4a" and "siV4b" mark two different siRNA constructs against TRPV4. ****P*<0.001.

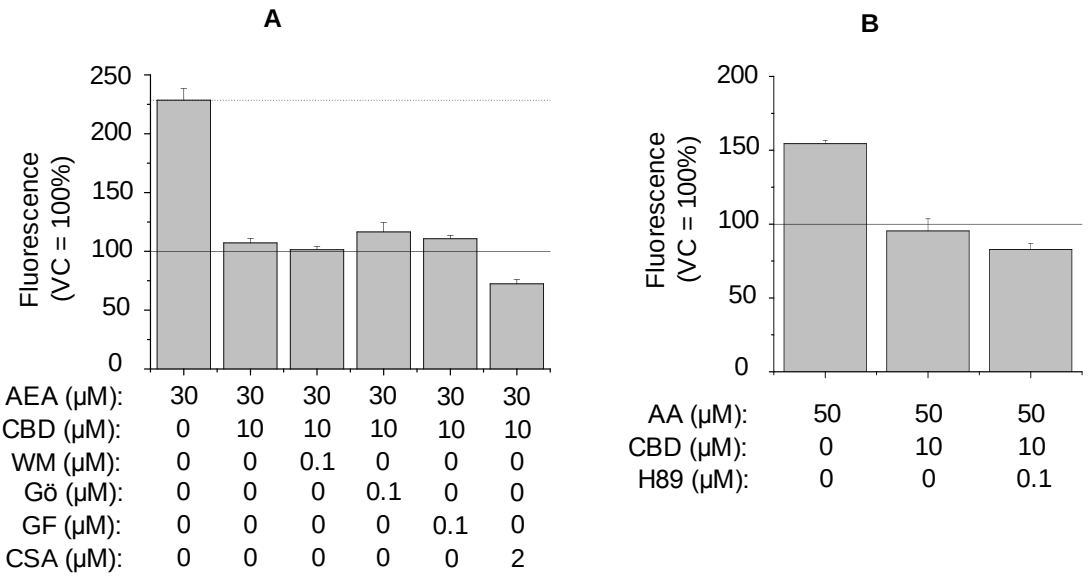

Supplemental Figure 11. *Lipostatic effect of CBD is not mediated by activation of PKC, PI3K, calcineurin (PP2B) or PKA*

Neutral lipid synthesis (Nile Red staining; 24-hr treatments) following various inhibitor treatments in combination with anandamide (**A**) or arachidonic acid (**B**). Data are expressed as mean±SEM of four independent determinations as the percentage of the vehicle control (100%, solid line). One additional experiment yielded similar results. AA: arachidonic acid, AEA: anandamide, CBD: cannabidiol, CSA: Cyclosporine A (inhibitor of calcineurin), GF: GF109203X (inhibitor of the conventional and novel PKC isoforms), Gö: Gö6976 (inhibitor of the conventional PKC isoforms), H89 (inhibitor of PKA), PKA: protein kinase A, PKC: protein kinase C, PI3K: phosphatidyl-inositol-3-kinase, PP2B: protein phosphatase 2B, WM: wortmannin (inhibitor of phosphatidyl-inositol-3-kinase).

Supplemental Figure 12. *Hierarchy of down-regulated Biological Networks Gene Ontology (BiNGO) terms following CBD treatment (10 μM, 24 hrs). Size of the nodes is proportional to the number of the identified genes of the corresponding GO term, whereas color of each node correlates to the adjusted P-value of the GO term (bigger size and more yellow color indicate higher number and significance, respectively)*

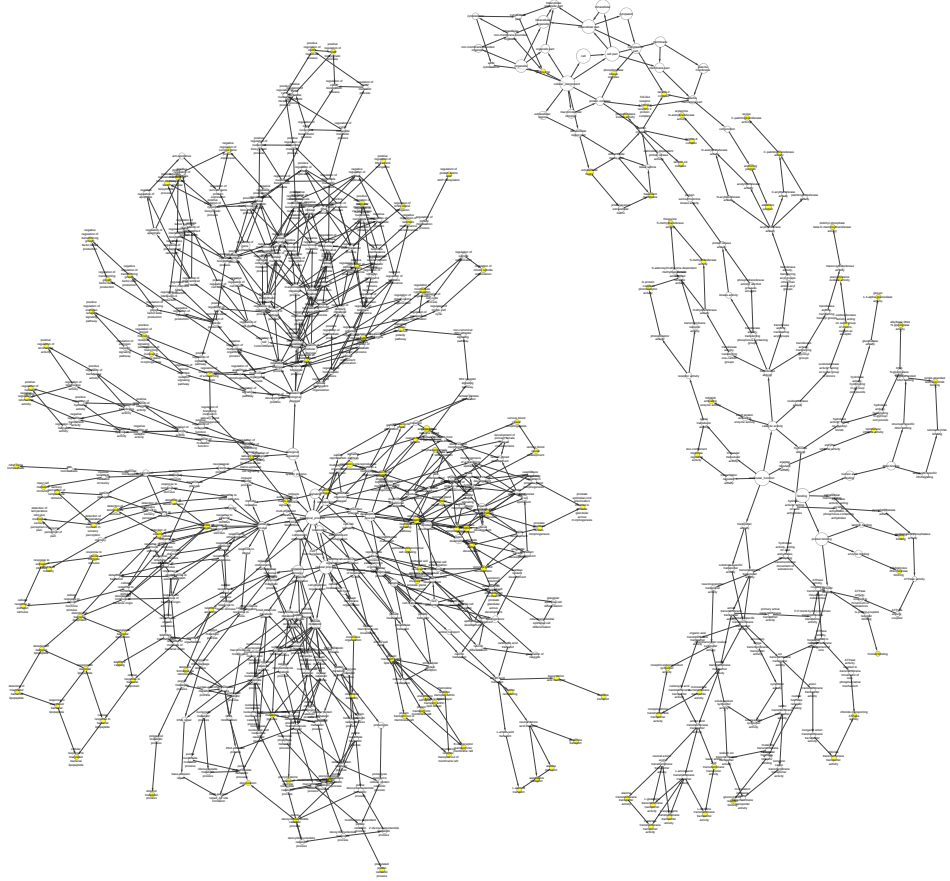

Supplemental Figure 13. *Hierarchy of up-regulated Biological Networks Gene Ontology terms following CBD treatment (10 µM, 24 hrs). Size of the nodes is proportional to the number of the identified genes of the corresponding GO term, whereas color of each node correlates to the adjusted P-value of the GO term (bigger size and more yellow color indicate higher number and significance, respectively)*

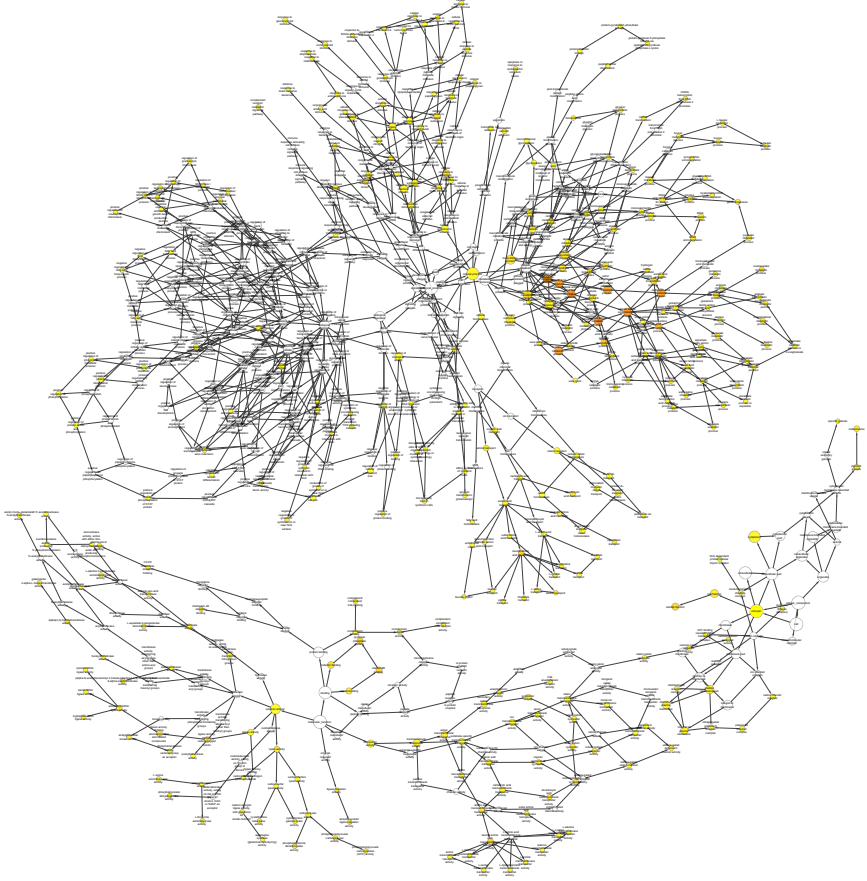

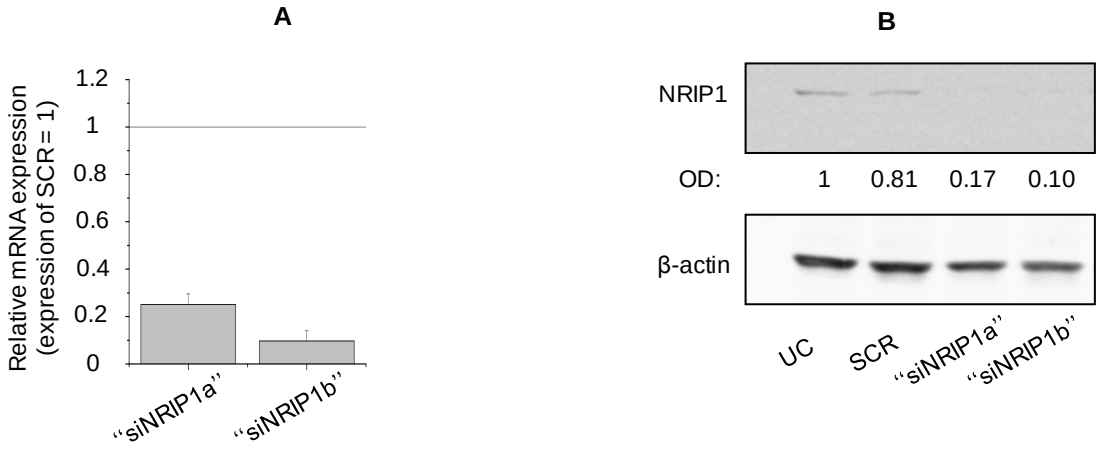

Supplemental Figure 14. *Evaluation of efficacy of selective gene silencing of NRIP1*

(**A**) *NRIP1* mRNA expression two days after selective gene silencing. Data are presented by using ΔΔCT method regarding peptidyl-prolyl isomerase A (*PPIA*) normalized *NRIP1* mRNA expression of the scrambled (SCR) control as 1 (solid line). Data are expressed as mean±SD of three independent determinations. (**B**) Western blot analysis of lysates of untransfected (UC), non-sense RNA transfected (SCR: scrambled control), and NRIP1-silenced SZ95 sebocytes three days after the transfection. OD: β-actin-normalized optical density of the corresponding bands. "siNRIP1a" and "siNRIP1b" mark two different constructs against NRIP1. NRIP1: nuclear receptor interacting protein-1.

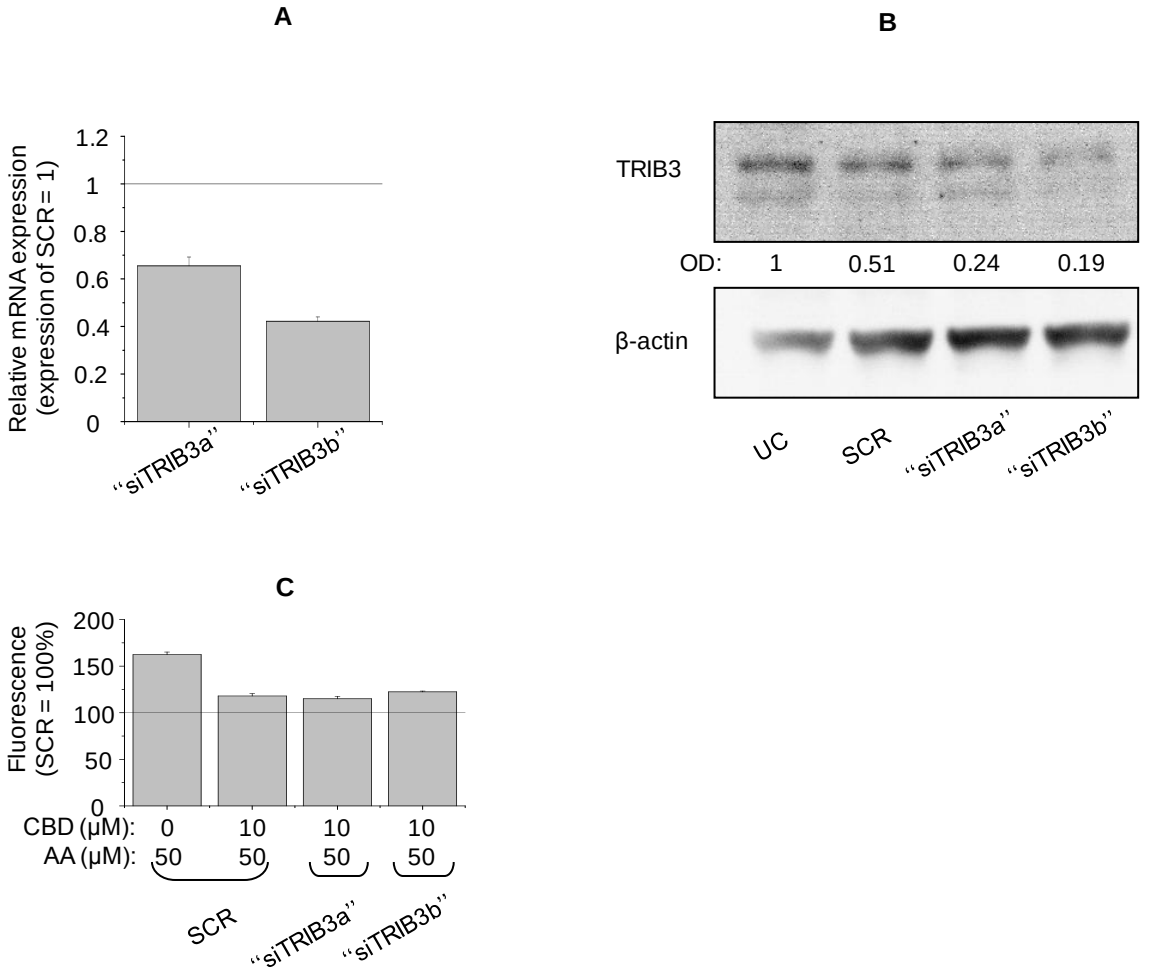

Supplemental Figure 15. *Evaluation of efficacy of selective gene silencing of TRIB3*

(**A**) *TRIB3* mRNA expression two days after selective gene silencing. Data are presented by using ΔΔCT method regarding peptidyl-prolyl isomerase A (*PPIA*) normalized *TRIB3* mRNA expression of the scrambled (SCR) control as 1 (solid line). Data are expressed as mean±SD of three independent determinations. (**B**) Western blot analysis of lysates of untransfected (UC), non-sense RNA transfected (SCR: scrambled control), and TRIB3-silenced SZ95 sebocytes two days after the transfection. OD: β-actin-normalized optical density of the corresponding bands. (**C**) Neutral lipid synthesis (Nile Red staining) following various treatments. Data are expressed as mean±SEM of four independent determinations as the percentage of the SCR vehicle control (100%, solid line). One additional experiment yielded similar results. "siTRIB3a" and "siTRIB3b" mark two different constructs against TRIB3. AA: arachidonic acid, CBD: cannabidiol, TRIB3: tribbles homolog 3.

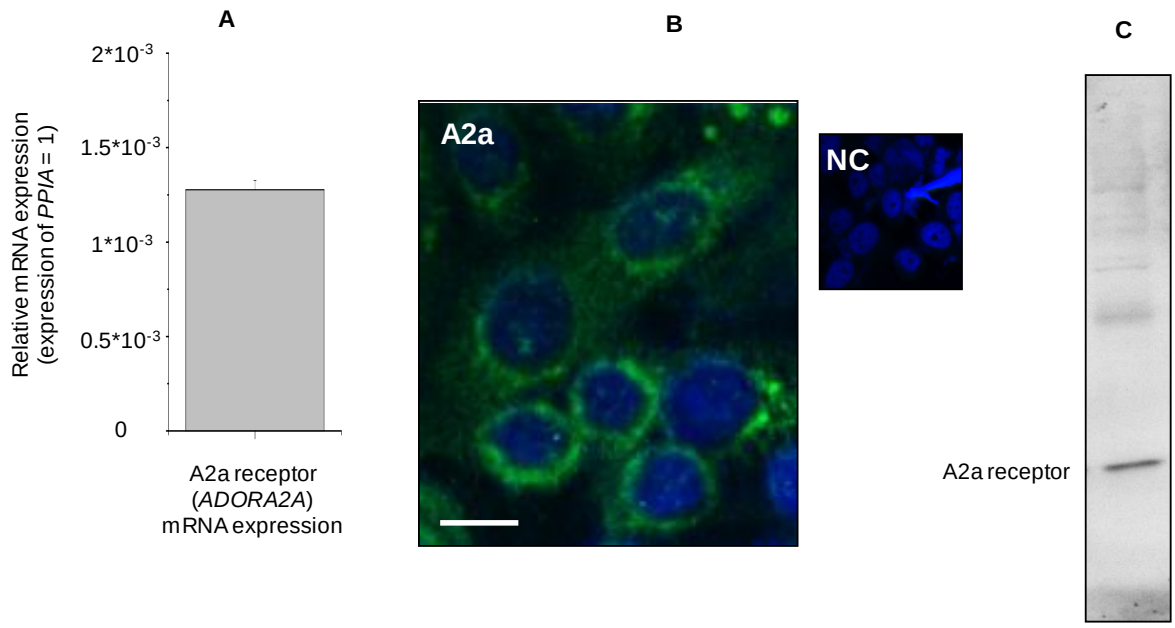

Supplemental Figure 16. *Human SZ95 sebocytes express adenosine A2a receptor*

(**A**) Quantitative "real time" PCR on SZ95 sebocyte samples harvested at 60% confluence. Data of A2a receptor (*ADORA2A*) mRNA expression was normalized to the level of *PPIA* of the same sample, and is expressed as mean±SD of three independent determinations. Two additional experiments yielded similar results. (**B**) Immunocytochemistry. A2a-specific immunreactivity was determined by immunofluorescence labeling (Alexa-Fluor®-488, green fluorescence) in SZ95 sebocytes. Nuclei were counterstained with DAPI (blue fluorescence). NC: negative control. Scale bar: 10 µm. (**C**) Western blot analysis of lysate of SZ95 sebocytes (~60% confluence culture).

5. Supplemental references

81. Juknat A, Rimmerman N, Levy R, et al. Cannabidiol affects the expression of genes involved in zinc homeostasis in BV-2 microglial cells. *Neurochem Int*. 2012;61(6):923-30.

82. Entrez Gene: http://www.ncbi.nlm.nih.gov/gene/23002
Accessed: July 5, 2013.

83. Hu Y, Ylivinkka I, Chen P, Li L, et al. Netrin-4 promotes glioblastoma cell proliferation through integrin β4 signaling. *Neoplasia.* 2012;14(3):219-27.

84. Entrez Gene: http://www.ncbi.nlm.nih.gov/gene/79689
Accessed: July 5, 2013.

85. Varley CL, Bacon EJ, Holder JC, Southgate J. FOXA1 and IRF-1 intermediary transcriptional regulators of PPARgamma-induced urothelial cytodifferentiation. *Cell Death Differ.* 2009;16(1):103-114.

86. Entrez Gene: http://www.ncbi.nlm.nih.gov/gene/7096
Accessed: July 5, 2013.

87. Schriever SC, Deutsch MJ, Adamski J, et al. Cellular signaling of amino acids towards mTORC1 activation in impaired human leucine catabolism. *J Nutr Biochem.* 2013;24(5):824-31.

88. Yang Y, Tarapore RS, Jarmel MH, et al. p53 mutation alters the effect of the esophageal tumor suppressor KLF5 on keratinocyte proliferation. *Cell Cycle.* 2012;11(21):4033-4039.

89. Rattner A, Hsieh JC, Smallwood PM, et al. A family of secreted proteins contains homology to the cysteine-rich ligand-binding domain of frizzled receptors. *Proc Natl Acad Sci U S A.* 1997;94(7):2859-2863.

90. Guha U, Mecklenburg L, Cowin P, et al. Bone morphogenetic protein signaling regulates postnatal hair follicle differentiation and cycling. *Am J Pathol.* 2004;165:729–740.

91. Entrez Gene: http://www.ncbi.nlm.nih.gov/gene/4288
Accessed: July 5, 2013.

92. Owen HR, Elser M, Cheung E, et al. MYBBP1a is a novel repressor of NF-kappaB. *J Mol Biol.* 2007;366(3):725-36.

93. Yabuta N, Onda H, Watanabe M, et al. Isolation and characterization of the TIGA genes, whose transcripts are induced by growth arrest. *Nucleic Acids Res.* 2006;34(17):4878-92.

94. Kim JM, Kosak JP, Kim JK, et al. NAG-1/GDF15 Transgenic Mouse Has Less White Adipose Tissue and a Reduced Inflammatory Response. *Mediators Inflamm.* 2013;2013:641851.